The polarity protein Scrib limits atherosclerosis development in mice

Schürmann, Christoph; Dienst, Franziska L; Pálfi, Katalin; Vasconez, Andrea E; Oo, James A; Wang, ShengPeng; Buchmann, Giulia K; Offermanns, Stefan; van de Sluis, Bart; Leisegang, Matthias S

Published in:
Cardiovascular Research

DOI:
10.1093/cvr/cvz093

Publication date:
2019

ESC European Society of Cardiology
Cardiovascular Research
doi:10.1093/cvr/cvz093

The polarity protein Scrib limits atherosclerosis development in mice

Christoph Schürmann[1,2]*, Franziska L. Dienst[1], Katalin Pálfi[1], Andrea E. Vasconez[1,2], James A. Oo [1,2], ShengPeng Wang[3], Giulia K. Buchmann [1,2], Stefan Offermanns[2,3], Bart van de Sluis[4], Matthias S. Leisegang[1,2], Stefan Günther[5], Patrick O. Humbert [6,7], Eunjee Lee[8,9], Jun Zhu [8,9], Andreas Weigert [10], Praveen Mathoor[10], Ilka Wittig[2,11], Christoph Kruse[1], and Ralf P. Brandes [1,2]*

[1]Institute for Cardiovascular Physiology, Goethe-University, Theodor-Stern Kai 7, Frankfurt, Frankfurt am Main 60590, Germany; [2]German Center for Cardiovascular Research (DZHK), Partner Site RheinMain, Theodor-Stern Kai 7, 60590 Frankfurt, Germany; [3]Department of Pharmacology, Max Planck Institute for Heart and Lung Research, Ludwigstrasse 43, 61231 Bad Nauheim, Germany; [4]Department of Pediatrics, Molecular Genetics Section, University of Groningen, University Medical Center Groningen, Antonius Deusinglaan 1, 9713 AV Groningen, The Netherlands; [5]ECCPS Bioinformatics and Sequencing Facility, Goethe-University, Ludwigstrasse 43, 61231 Bad Nauheim, Germany; [6]Department of Biochemistry & Genetics, La Trobe Institute for Molecular Science, La Trobe University, Kingsbury Drive, Melbourne, Victoria, 3086, Australia; [7]Department of Clinical Pathology, Department of Molecular Biology and Biochemistry, The University of Melbourne, Grattan Street, Parkville, Victoria, 3010, Australia; [8]Icahn School of Medicine at Mount Sinai, 1 Gustave L. Levy Pl, New York, NY 10029, USA; [9]Sema4 Genomics, a Mount Sinai Venture, 333 Ludlow Street, South tower 3rd floor, Stamford, CT 06902, USA; [10]Institute of Biochemistry I–Pathobiochemistry, Goethe-University, Frankfurt, Theodor-Stern Kai 7, 60590 Frankfurt am Main, Germany; and [11]Functional Proteomics, SFB815 Core Unit, Medical School, Goethe University, Frankfurt, Theodor-Stern Kai 7, 60590 Frankfurt am Main, Germany

Received 26 September 2018; revised 27 February 2019; editorial decision 31 March 2019; accepted 2 April 2019

Time for primary review: 28 days

Aims The protein Scrib (Scribble 1) is known to control apico-basal polarity in epithelial cells. The role of polarity proteins in the vascular system remains poorly characterized; however, we previously reported that Scrib maintains the endothelial phenotype and directed migration. On this basis, we hypothesized that Scrib has anti-atherosclerotic functions.

Methods and results Tamoxifen-induced Scrib-knockout mice were crossed with ApoE$^{-/-}$ knockout mice and spontaneous atherosclerosis under high-fat diet (HFD), as well as accelerated atherosclerosis in response to partial carotid artery ligation and HFD, was induced. Deletion of Scrib resulted in increased atherosclerosis development in both models. Mechanistically, flow- as well as acetylcholine-induced endothelium-dependent relaxation and AKT phosphorylation was reduced by deletion of Scrib, whereas vascular permeability and leucocyte extravasation were increased after Scrib knockout. Scrib immune pull down in primary carotid endothelial cells and mass spectrometry identified Arhgef7 (Rho Guanine Nucleotide Exchange Factor 7, βPix) as interaction partner. Scrib or Arhgef7 down-regulation by siRNA reduced the endothelial barrier function in human umbilical vein endothelial cells. Gene expression analysis from murine samples and from human biobank material of carotid endarterectomies indicated that loss of Scrib resulted in endothelial dedifferentiation with a decreased expression of endothelial signature genes.

Conclusions By maintaining a quiescent endothelial phenotype, the polarity protein Scrib elicits anti-atherosclerotic functions.

Keywords Scribble 1 • Vascular reactivity • Atherosclerosis • Permeability • Inflammation

1. Introduction

Polarization is a typical feature of cells localized at interfaces. Epithelial cells exhibit apico-basal polarity to allow directed transport and specific positioning of junction proteins. Monolayer-forming cells also exhibit planar cell polarity, wherein intercellular communication promotes organelle positioning, the formation of a confluent monolayer, 2D-migration and control of cell proliferation.[1] Interestingly, in the vascular system shear stress-initiated signalling and its subsequent impact on endothelial function depend on planar cell polarity.[2] Typical examples for apico-basal polarity include the cells of the proximal tubule in the kidney. These express the Na/K-ATPase at the basal portion, the sodium-glucose

* Corresponding authors. Tel: +49 69 6301 85321; fax: +49 69 6301 7668, E-mail: brandes@vrc.uni-franfurt.de (R.P.B.); or Tel: +49 69 6301 85321; fax: +49 69 6301 7668, E-mail: schuermann@vrc.uni-frankfurt.de (C.S.)

symporter at the apical site and the tight junctions towards the apical portion of the lateral cell membrane. This positioning of proteins is achieved through a localized activation of kinases and small GTPases like Rac1 and CDC42.[3] Distinct protein complexes control the individual forms of polarity, although a certain degree of crosstalk is present as lateral junctions contribute to both functions. These complexes form three groups: At the apico-lateral side, the Par complex [Par3 (PARD3)/Par6 (PARD6)/aPKC] and the Crumbs [Crumbs (CRB1, 2, 3)/Pals1 (MPP5)/Patj] complex reside, whereas the Scribble complex [Scrib, Lgl (LLGL1-2), Dlg (DLG1-4)] is localized at the basolateral region.[4]

Vascular endothelial cells, which form the inner-most layer of blood vessels, are also polarized.[5] Endothelial cells attach to the basal lamina through integrins, while lateral adhesion complexes connect cells to maintain the monolayer. Basal and lateral connections, not only provide stability, but they also inform endothelial cells about their orientation. Integrin signalling from the basal lamina provides apico-basal orientation, whereas lateral orientation comes from junctional molecules. Moreover, biomechanical sensing in endothelial cells depends on basal and lateral cues including integrin or lateral junction disruption, stretch and flow. Disruption of endothelial lateral junction complexes, for example by mutation or knockdown of VE-cadherin or PECAM-1, attenuates endothelial flow sensing and flow-induced nitric oxide (NO) production and vasodilatation.[6]

In comparison to epithelial cells, the role of the polarity protein Scrib in endothelial cells is largely uncharacterized. We have previously shown that Scrib is involved in endothelial-directed cell migration and angiogenesis by controlling integrin trafficking.[7] Moreover, Scrib had a permissive effect on endothelial cell inflammatory signalling by controlling the abundance of the transcription factor GATA-like protein 1.[5] Atherosclerosis is promoted by inflammation and endothelial dysfunction (two aspects of vascular biology already demonstrated to be affected by Scrib). In the present study, we set out to determine the role of Scrib in atherosclerosis development in two different mouse models and determined the underlying mechanisms.

2. Methods

TOP Guideline statement: The data that support the findings of this study are available from the corresponding authors upon reasonable request.

2.1 Animal model

All animal experiments were performed in accordance with the National Institutes of Health Guidelines on the Use of Laboratory Animals. The University Animal Care Committee and the Federal Authorities for Animal Research (Darmstadt, Germany) approved the study protocol. Mice were bred at the local facility under standard conditions with a 12/12 h dark-light cycle and free access to chow and water. Mice used for the experiments were caged with blinded identity and random orders.

2.2 *In vivo* Scrib knockout

Scrib flox/flox mice were generated by one of the co-authors (P.O.H.).[8] Cdh5-CreERT2 mice were kindly provided by Ralf Adams, MPI Münster. The general characterization of tamoxifen-inducible endothelial-specific Scrib*/* mice (Scrib1-flox/flox-CDH5-Cre-ERT2) has been described previously.[5] Tamoxifen-inducible global ApoE Scrib*/* mice (ApoE$^{-/-}$ Scrib1-flox/flox-rosa-Cre-ERT2) were produced by crossing Scrib1 flox/flox mice with Cre-ERT2$^{+/0}$ ApoE$^{-/-}$ mice. Genomic recombination was achieved by oral tamoxifen administration with the chow (LASCRdiet CreActive TAM400, LASvendi, Soest, Germany) for five consecutive days followed by 2 days of normal chow, an additional five consecutive days of tamoxifen administration and a 'wash-out' phase of 2 weeks. In all *in vivo* experiments, Cre positive (Cre$^{+/0}$) and Cre negative (Cre$^{0/0}$) control animals received tamoxifen, animals were sacrificed using Isoflurane and cervical dislocation. Animals were 6–7 weeks of age, male and of the C57BL/6 background.

2.3 High-fat diet-induced atherosclerosis model

The role of Scrib in spontaneous atherosclerosis development in ApoE background mice was determined after 2 months of high-fat diet (HFD). Animals received tamoxifen treatment and a 'wash-out' phase. At the age of 10 weeks, mice began a high-fat, cholesterol-rich diet that contained 21% fat, 19.5% casein, and 1.25% cholesterol (Ssniff, Soest, Germany).[9]

2.4 Partial left common carotid artery ligation model

Western-type (42% of total calories from fat, 1.5% cholesterol) diet was purchased from Ssniff (Soest, Germany). Animals were started on the western-type diet after tamoxifen treatment and 'wash-out' phase at an age of 10 weeks. Neo-intima formation and accelerated atherosclerosis was induced 4 days later by partial left common carotid artery ligation as described previously.[10] In brief, mice were anaesthetized using intraperitoneal injection of xylazine (5 mg/kg) and ketamine (100 mg/kg). The skin was shaved, disinfected (Braunol, B.Braun, Melsungen, Germany) and a ventral midline incision (5 mm) was made in the neck. The left common carotid artery was exposed by blunt dissection. Excepting the superior thyroid artery, the left internal and external carotid and the occipital artery were ligated with 6–0 silk suture. The incision was closed and the mice received subcutaneous injections of buprenorphine (0.05 mg/kg) post-surgery and every 12 h thereafter for the following 3 days.

2.5 Permeability assays

For the mouse ear swelling assay, croton oil (10 µL, 1% in acetone, Sigma-Aldrich, Zwijndrecht, the Netherlands) was topically applied to the anterior surfaces of the left ear. The right ear (control) received the vehicle (acetone). Swelling of the ear was allowed to develop for 24 h, after which the ear thickness was measured using a digimatic thickness gage (No. 547-401, Mitutoyo, Takatsu-ku, Japan). Lung permeability and macrophage extravasation were studied with and without lipopolysaccharides (LPS, *Escherichia coli* 0111: B4, 8 mg/kg, i.p., dissolved in 0.9% saline). Pulmonary extravasation was determined with Evans blue dye (1% in NaCl 0.9%). The dye was injected intravenously and after 15 min, animals were sacrificed and the lungs were removed and mortared after snap freezing. Evans blue was extracted with dimethylformamide (2 mL/lung) and the samples subsequently cleared by centrifugation. The fluorescence of Evans blue was measured against a standard curve (excitation 600 nm, emission 680 nm) in a TECAN micro-plate reader (Infinite M200Pro, TECAN, Männedorf, Switzerland).

2.6 Vascular reactivity studies

Vascular reactivity studies were performed as described previously.[11] Mouse mesenteric artery rings were suspended between two stainless steel triangles in a heated organ chamber setup and passively stretched to 0.6 g for isometric tension recordings. Following two initial

contractions to potassium chloride (80 mmol/L), cumulative dose-response curves to the alpha-adrenergic constrictor phenylephrine and the endothelium-dependent vasodilator acetylcholine (ACh) were generated with and without inhibition of the NO synthase with N^{ω}-nitro-L-arginine (L-NA).

2.7 Pressure myography studies

Pressure myography studies were performed as described previously.[12] Arteries of the 3rd or 4th branch were removed from the mesentery and used for the measurements in a chamber (Danish Myo Technology, Aarhus, Denmark). The external diameter of the artery was visualized and recorded. After reaching a steady-state diameter, vessels were contracted with 50–150 nM U46619 to 40–50% of the passive diameter or by increasing of the intravascular pressure to 75–90 mmHg to induce myogenic contraction. After reaching a stable baseline, flow was increased in a stepwise manner by changing the pressure of the inflow and outflow side inversely, thereby creating a pressure difference across the arteriole without altering the intraluminal pressure. The viability of the vessel was verified at the end of the experiment by dilation of the vessel with acetylcholine (10 µM) or sodium nitroprusside (100 µM). Vasodilatation to flow was calculated as a percentage of the U46619-induced contraction as described previously.[13]

2.8 Cell culture

Endothelial cells isolated from the murine carotid artery (CEC)[14] of $ApoE^{-/-}$ and ApoE Scrib*/* mice were cultured on gelatin-coated (Merck, Darmstadt, Germany) dishes in endothelial growth medium, consisting of DMEM/F12 (Thermo Fisher Scientific, Dreieich, Germany) supplemented with EndoCGS-Heparin, (PELOBiotech, Planegg, Germany), 20% foetal calf serum (FCS) (#S0113, Biochrom, Berlin, Germany), penicillin (50 U/ml), and streptomycin (50 µg/ml) [#15140-122, Gibco (Life Technologies, Carlsbad, CA, USA)] in a humidified atmosphere of 5% CO_2 at 37°C. For each experiment at least three different isolates were used. The CECs were used between passages 5–9. Scrib KO was induced with 4-Hydroxytamoxifen (OH-Tam., 1 µM, 2 days, Sigma-Aldrich, München, Germany).

In some experiments, cells were starved (0.5% FCS, 5 h) and subsequently subjected to continuous arterial laminar flow generated by a customized cone–plate viscometer (12 dyne/cm^2). In other experiments, CEC were starved (0.5% FCS, 4 h) and subsequently exposed to the PIEZO-channel activator Yoda1 (1 µmol/L, 5 or 20 min) or to insulin (0.1 and 1 µmol/L, 15 min) with or without pre-incubation (30 min) with the phosphatidylinositide 3-kinase inhibitor Ly29004 (10 µmol/L).

Human umbilical vein endothelial cells (HUVEC) were purchased from Lonza (Walkersville, MD). Cells were cultured in EBM (Lonza, Walkersville, MD) supplemented with 10% FCS, bovine brain supplement and human recombinant EGF, penicillin (50 U/ml) and streptomycin (50 µg/ml). Third passage endothelial cells were used throughout.

For siRNA treatment, endothelial cells (80–90% confluent) were transfected with siRNA using GeneTrans II according to MoBiTec (Göttingen, Germany) instructions. Scrambled (Scr), Scrib and Arhgef7 siRNAs (Invitrogen, Darmstadt, Germany) were used for experiments. Two days after transfection the impedance measurements were performed.

2.9 *In vitro* permeability assay

In vitro permeability was assessed with CEC monolayers grown in 12-well cell culture inserts with a semipermeable membrane (3 µm, BD Bioscience, Allschwil, Switzerland) using fluorescein rhodamine isothiocyanate-dextran (20 mg/mL, R9379, Sigma-Aldrich, München, Germany). Measurements were performed with an excitation wavelength of 510 nm and an emission wavelength of 580 nm using a TECAN micro-plate reader (Infinite M200Pro, TECAN, Männedorf, Switzerland).

2.10 Isolation of mRNA and PCR

Organs were removed, snap frozen in liquid nitrogen and mortared. Total mRNA was isolated from tissue or primary endothelial cells with the Bio&Sell RNA-Minikit (Bio&Sell, Feucht, Germany) according to the manufacturer's instructions. cDNA synthesis was carried out using SuperScript III Reverse Transcriptase (Invitrogen, Carlsbad, CA, USA) random hexamer primers with oligo(dT) primers, real-time PCR was performed with Eva Green Master Mix and ROX as reference dye (Thermo Scientific) in an Mx4000 cycler (Stratagene). Relative expressions of target genes were normalized to eukaryotic translation elongation factor 2 (EF2), analysed by delta-delta-CT method. The following primers were used: EF2_F: 5′-GACATCACCAAGGGTGTGCAG-3′, EF2_R: 5′-GCGGTCAGCACACTGGCATA-3′, eNOS_F: 5′- CTCA CCATAGCTGTGCTGGCTTAC-3′, eNOS_R: 5′- GATGCAGGGC AAGTTAGGATCAGG-3′, Rosa_Cre_F: 5′-AAAGTCGCTCTGA GTTGTTAT-3′, Rosa_Cre_F2: 5′-GGAGCGGGAGAAATGGATATG-3′, Emr1_F: 5′-TGGATGCTAGTGGAGGCAGTGATG-3′, Emr1_R: 5′-GCAATGGCCTTGAAGGTCAGCAAC-3′, Mmp3_F: 5′-GGGAAG CTGGACTCCAACAC-3′, Mmp3_R: 5′-GCGAACCTGGGAAGGTA CTG-3′, Pkdcc_F: 5′-ACAGTGAGGGCATCCCAGAC-3′, Pkdcc_R: 5′-GCCAAGGCTGAGGCAGATTC-3′, Rosa_Cre_R: 5′-CCTGATCC TGGCAATTTCG-3′, Rspo3_F: 5′-TTGCCCAGAAGGGTTAGAAG-3′, Rspo3_R: 5′-TTGGCTGAAGGATGCTGTAG-3′, Scrib_flox_F: 5′-TGCTTTCTCCCAGACTCAGG-3′, Scrib_flox_R: 5′-GCCATGGTGG CAGAGGTTGG-3′, Sfrp2_F: 5′-ACGGCATCGAGTACCAGAAC-3′, Sfrp2_R: 5′-GCGAGCACAGGAACTTCTTG-3′.

2.11 RNA-sequencing

Total RNA was isolated from murine carotid endothelial cells (CEC) of endothelial-specific Scrib*/* mice (Scrib1-flox/flox-CDH5-Cre-ERT2) as described before. To remove possible genomic DNA contamination, samples were treated with DNase by on-column digestion (DNase-Free DNase Set, Qiagen, Hilden, Germany). Total RNA and library integrity were verified with LabChip Gx Touch 24 (Perkin Elmer, Rodgau, Germany). One microgram of total RNA was used as input for SMARTer Stranded Total RNA Sample Prep Kit—HI Mammalian (Clontech, Mountain View, CA, USA). Sequencing was performed on the NextSeq500 instrument (Illumina, San Diego, CA, USA) using v2 chemistry, resulting in an average of 40 M reads per library with 1 × 75 bp single end set-up. The resulting raw reads were assessed for quality, adapter content, and duplication rates with FastQC (http://www.bioinformatics.babraham.ac.uk/projects/fastqc/). Reaper version 13-100 was employed to trim reads after a quality drop below a mean of Q20 in a window of 10 nucleotides.[15] Only reads between 30 and 150 nucleotides were cleared for further analyses. Trimmed and filtered reads were aligned against the Ensembl mouse genome version mm10 (GRCm38) using STAR 2.4.0a with the parameter '-outFilterMismatchNoverLmax 0.1' to increase the maximum ratio of mismatches to mapped length to 10%.[16] The number of reads aligning to genes was counted with featureCounts 1.4.5-p1 tool from the Subread package.[17] Only reads mapping at least partially inside exons were admitted and aggregated per gene. Reads overlapping multiple genes or aligning to multiple regions

were excluded. Differentially expressed genes were identified using DESeq2 version 1.62.[18] Only genes with a maximum Benjamini–Hochberg corrected *P*-value of 0.05, and a minimum combined mean of 10 reads were deemed to be significantly differentially expressed. The Ensemble annotation was enriched with UniProt data (release 06.06.2014) based on Ensembl gene identifiers [Activities at the Universal Protein Resource (UniProt)].

2.12 Plasma lipid parameters

Lipoprotein profiles were determined on plasma samples from mice using an ÄKTA Basic chromatography system with a Superose 6PC 3.2/30 column (Amersham Biosciences, Roosendaal, the Netherlands) as described previously in detail.[19] After collection, the samples were kept on ice, centrifugated at 4°C for 15 min at 800 rpm and snap frozen in liquid nitrogen. Plasma cholesterol and triglyceride level were measured using a commercially available kit (1489232, Chol CHOD-PAP, Roche, Almere, the Netherlands, 337-B, TG GPO-trinder, Sigma-Aldrich, Zwijndrecht, the Netherlands). Measurements were performed according to manufacturer's protocols on a Benchmark 550 nm micro-plate reader (170-6750XTU, Bio-Rad, Veenendaal, the Netherlands).

2.13 Immunoblotting

Western blot analyses were performed with an infrared-based detection system (Odyssey, Licor, Bad Homburg, Germany) using the following primary antibodies: Santa Cruz (Heidelberg, Germany): Anti-Scrib (#sc-11048), Cell Signaling (Danvers, MA; USA): Anti-Akt, phospho-Ser473- (#4058S), anti-AKT (#2920), Sigma-Aldrich (München, Germany): anti-beta-Actin (#A1978). Cells were lysed with Triton X-100 lysis buffer [20 mM TRIS/Cl pH 7.5, 150 mM NaCl, 10 mM NaPPi, 20 mM NaF, 1% triton, 2 mM ortho-vanadat (OV), 10 nM okadaic acid, protein-inhibitor mix (PIM, Roche, Basel, Switzerland), 40 µg/ml phenylmethylsulfonyl fluoride]. Protein concentration was determined by Bradford protein assay (Pierce) and samples containing 10–30 µg protein were subjected to SDS-PAGE followed by western blot. Infrared-fluorescent-dye-conjugated secondary antibodies (Licor, Bad Homburg, Germany) were used to detect primary antibodies and visualization was carried out with a Licor infrared scanner (Licor, Bad Homburg, Germany).

2.14 Immunohistochemistry

After partial ligation of the carotid artery of mice, animals were sacrificed and perfused transcardially with vasodilation buffer [5 min; phosphate buffered saline (PBS), papaverine 4 mg/L, adenosine 1 g/L; Sigma-Aldrich, Taufkirchen, Germany] followed by intravascular paraformaldehyde fixation (15 min; 4% PFA; Roth, Karlsruhe, Germany) and embedding in paraffin. Serial sectioning (4 µm), from close to the aortic arch to the bifurcation (500 µm steps), was performed on the left and right carotid artery after harvesting on postoperative day 28. Sections were counterstained with haematoxylin and eosin (H/E). The lumen of the carotid artery was determined by planimetry with the aid of the NIH-ImageJ software.

The brachiocephalic trunk was fixed in 4% PFA, dehydrated in 30% sucrose and embedded in Tissue-Tek O.C.T. Five sections (10 µm slides) were cut sequentially every 50 µm from the aortic arch to the bifurcation. Histological slides were stained with Oil red O. To determine aSMA or macrophage content, cross-sections of brachiocephalic trunk were stained. After fixation in acetone, tissue was blocked with 5% goat serum in PBS, followed by incubation with anti-aSMA (C6198, Sigma-Aldrich, Germany), anti-ERG1 (ab92513, Abcam, Berlin, Germany), and anti-Moma2 (ab33451, Abcam, Berlin, Germany) antibodies and appropriate fluorescence coupled secondary antibody. Subsequently, images were obtained by confocal microscopy on a Zeiss LSM 800. Specificity of staining was controlled by incubation with the detection antibody alone.

2.15 Cell electric impedance measurement

xCELLigence RTCA DP system (OLS—OMNI Life Science GmbH) was used according to the manufacturer's instructions.

2.16 Co-immunoprecipitation and mass spectrometry

For immunoprecipitation of Scrib with an anti-Scrib antibody (Santa Cruz, #sc-11048), carotid artery endothelial cells of endothelial-specific Scrib*/* mice (Scrib1-flox/flox-CDH5-Cre-ERT2$^{+/0}$) cells were used. Cells were isolated and subsequently treated with 4-hydroxytamoxifen as described before and lysed in lysis buffer (75 mM Tris/HCl, pH 7.5, 200 mM NaCl, 15 mM NaF, 7.5 mM EGTA, 7.5 mM EDTA, 0.5% TritonX100, 0.25% Nonident NP40, 2 mM orthovanadate, and protein-inhibitor mixture). Three days after induction of the knockout supernatants of the cellular extracts were incubated with anti-Scrib antibody (3 µg) over night at 4°C followed by incubation for an additional 2 h with Protein G-Magnetic beads (Invitrogen). Subsequently, beads were extracted on the magnetic column and washed with lysis buffer with 0.1% detergent without inhibitors and another two times with wash buffer (20 mM Tris/HCl, pH 7.4, 200 mM NaCl).

Sample preparation for mass spectrometry: Beads were dissolved in 6 M Guanidinhydrochlorid (GdmCl), 50 mM Tris/HCl, pH 8.5, 10 mM TCEP and incubated at 95°C for 5 min. Reduced thiols were alkylated with 40 mM chloroacetamid and samples were diluted with 25 mM Tris/HCl, pH 8.5, 10% acetonitrile to obtain a final GdmCl concentration of 0.6 M. Proteins were digested with 1 µg Trypsin (sequencing grade, Promega) overnight at 37°C under gentle agitation. Digestion was stopped by adding trifluoroacetic acid to a final concentration of 0.5%. Peptides were loaded on multi-stop-and-go tip (StageTip) as described.[20] Four fractions from SCX stage tips were collected in wells of microtiter plates and peptides were dried and resolved in 1% acetonitrile, 0.1% formic acid. Mass spectrometry: Liquid chromatography/mass spectrometry (LC/MS) was performed on Thermo Scientific™ Q Exactive Plus equipped with an ultra-high performance liquid chromatography unit (Thermo Scientific Dionex Ultimate 3000) and a Nanospray Flex Ion-Source (Thermo Scientific). Peptides were loaded on a C18 reversed-phase precolumn (Thermo Scientific) followed by separation with 2.4 µm Reprosil C18 resin (Dr. Maisch GmbH) in-house packed picotip emitter tip (diameter 100 µm, 15 cm from New Objectives) using a gradient from 4% acetonitrile, 0.1% formic acid to 40% eluent B (99% acetonitrile, 0.1% formic acid) for 30 min with a flow rate 400 nL/min followed by an second gradient to 60% B for additional 5 min.

MS data were recorded by data dependent acquisition. The full MS scan range was 300–2000 m/z with resolution of 70 000, and an automatic gain control (AGC) value of 3*E6 total ion counts with a maximal ion injection time of 160 ms. Only higher charged ions (2+) were selected for MS/MS scans with a resolution of 17 500, an isolation window of 2 m/z and an AGC value set to 1*E5 ions with a maximal ion injection time of 150 ms. MS1-Data were acquired in profile mode.

MS Data were analysed by MaxQuant (v1.6.1.0)[21] using default settings. Proteins were identified using reviewed mouse reference proteome database UniProtKB with 16 997 entries, released in December

2018. The enzyme specificity was set to Trypsin. Acetylation (+42.01) at N-terminus and oxidation of methionine (+15.99) were selected as variable modifications and carbamidomethylation (+57.02) as fixed modification on cysteines. False discovery rate for the identification of proteins and peptides was 1%. Lable free quantification and intensity-based absolute quantification values were recorded. Data were further analysed by Perseus (v. 1.6.1.3). Contaminants and reversed identification were removed. Protein identification with at least three valid quantification values in at least one group were further analysed. Missing values were replaced by background values from normal distribution. Student's *t*-test was used to identify significant enriched proteins between experimental groups (C57, $n = 4$; Scrib */*, $n = 4$).

2.17 Biobank-of-Karolinska-Endarterectomy data

mRNA expression data of human carotid atherosclerotic plaque were retrieved from the Biobank Each (BiKE) and downloaded (GSE21545).[22] For correlation analysis of gene expression comparing Scrib and other genes, the Pearson correlation coefficient was calculated in R using the cor.test function.

2.18 Statistical analyses

Unless otherwise indicated, data are given as means ± standard error of the mean (SEM). Calculations were performed with Prism 5.0, R or BiAS.10.12. The latter was also used to test for normal distribution and similarity of variance. In the case of multiple testing, Bonferroni correction was applied. For multiple group comparisons analysis of variance (ANOVA) followed by post-hoc testing was performed. Individual statistics of dependent samples were performed by paired *t*-test, of unpaired samples by unpaired *t*-test and, if not normally distributed, by Mann–Whitney test. *P*-values of <0.05 were considered as significant. Unless otherwise indicated, *n* indicates the number of individual experiments.

3. Results

3.1 Deletion of Scrib promotes atherosclerosis development

As a model for atherosclerosis development, ApoE$^{-/-}$ mice were subjected to a HFD. Tamoxifen administration to ApoE$^{-/-}$ Scrib1-flox/flox-rosa-Cre-ERT2$^{+/0}$ (denoted as Scrib*/*) mice compared with ApoE$^{-/-}$ Scrib1-flox/flox-rosa-Cre-ERT2$^{\circ/0}$ mice (denoted as ApoE) resulted in a robust loss of Scrib protein expression as detected by western blot (Supplementary material online, *Figure SIA*). Lipid levels and lipid profiles between ApoE$^{-/-}$ and Scrib*/* mice were similar (Supplementary material online, *Figure SIB, C*).

The degree of atherosclerosis development in the brachiocephalic trunk was determined after 2 months of HFD. Genetic deletion of Scrib almost doubled plaque load in this vessel (*Figure* 1A). Histological analysis

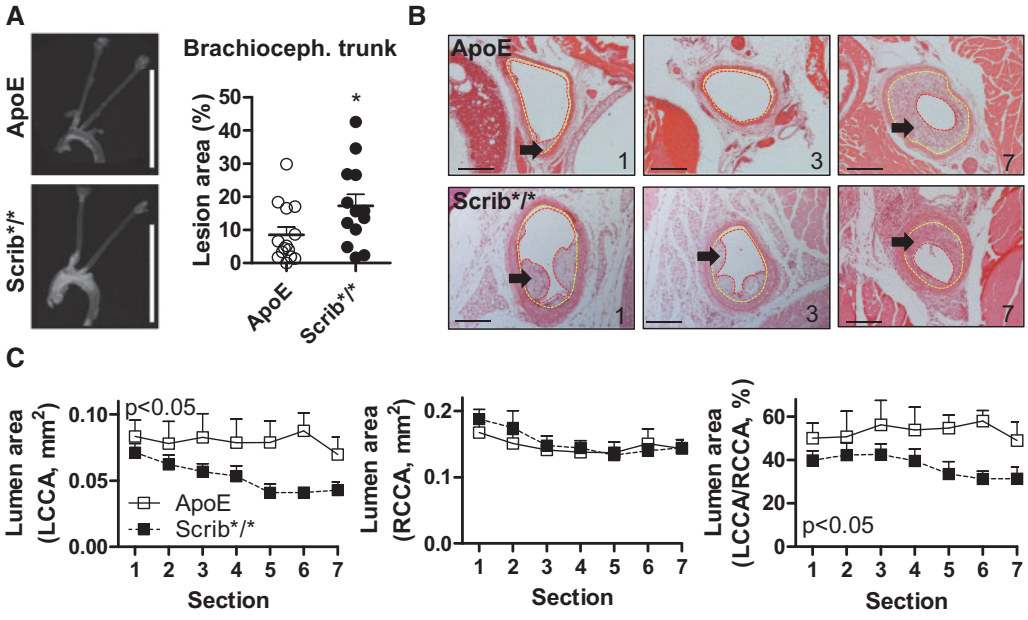

Figure 1 Role of Scrib for atherosclerosis development. (*A*) Role of Scrib in HFD-induced atherosclerosis. Representative photographs of the naïve aortic arch with carotid arteries and statistics of the planimetry of the brachiocephalic trunk, $n = 14$ ApoE$^{-/-}$ Scrib1-flox/flox-rosa-Cre-ERT2$^{0/0}$ (ApoE), $n = 13$ ApoE$^{-/-}$ Scrib1-flox/flox-rosa-Cre-ERT2$^{+/0}$ (Scrib*/*). Lesion area was determined by threshold-based planimetry of naïve brachiocephalic trunk. Scale bars are 20 mm. Tissue was collected after 2 months of HFD at 18 weeks of age; $^*P \leq 0.05$ as determined by *T*-Test. (*B, C*) Role of Scrib in accelerated plaque formation after partial carotid artery ligation and HFD. (*B*) Representative H&E stained cross section of the left operated common carotid artery of a ApoE and Scrib*/* mouse 28 days after partial carotid artery ligation. Seven sections were cut sequentially every 500 µm from the aortic arch (1) to the bifurcation (7). Section numbers 1, 3, and 7 are shown for ApoE and ApoE Scrib*/* mouse. Inner layer of the tunica media (yellow) and tunica intima (red) are marked. Arrows point to atherosclerotic plaques. Scale bars are 100 µm. (*C*) Quantitative 2D histology with vascular lumen profile of the operated left common carotid artery (LCCA), non-operated right common carotid artery (RCCA), and normalization to the non-operated vessels according to the segmentation, $n = 7$ ApoE, 12 ApoE Scrib*/*. Data represent the means ± SEM; $^*P \leq 0.05$ as determined by ANOVA with Bonferroni's post-hoc test.

of the brachiocephalic trunk confirmed a significantly increased plaque burden in Scrib*/* mice compared with ApoE knockout animals (Supplementary material online, *Figure SIIA*), neutral lipid deposition and macrophage content (Moma2) and aSMA deposition were not different between the two mouse strains (Supplementary material online, *Figure SIIB, C*).To support the finding of a potential anti-atherosclerotic function of Scrib, a second atherosclerosis model was used: partial carotid artery ligation in ApoE mice subjected to western diet. In this model, a reduced blood flow accelerates atherosclerosis development. Morphometric analyses were performed 4 weeks after surgery using quantitative histology. Additionally, Scrib deletion in this model, resulted in a significant increase in the degree of atherosclerosis as indicated by increased lumen loss in the knockout mice compared with the control ApoE mice (*Figure* 1B, C). The non-operated right common carotid arteries did not differ between either strain. Plaque composition was not different between the two mouse strains, which was also true for cholesterol clefts, plaque haemorrhages and necrotic core size (data not shown). There was, however, a trend towards enhanced collagen and aSMA deposition and reduced endothelial cell count in lesions of Scrib*/* animals (Supplementary material online, *Figure SIII*).

3.2 Scrib facilitates vascular flow sensing

Release of protective autacoids, in particular NO, is considered the most important anti-atherosclerotic function of the endothelium. It is well known that human atherosclerosis develops at sites of low flow and thus low NO production and that flow-induced endothelium-dependent vasodilatation is attenuated in dysfunctional endothelium.[23] For this reason, the role of Scrib in flow-induced vasodilatation was tested. The genetic deletion of Scrib significantly reduced flow-induced dilatation of the isolated mesenteric artery of ApoE mice (*Figure* 2A).

Shear stress-stimulated NO release is a complex process. Phosphorylation of eNOS at serine 1177 by the Serine/threonine protein kinase Akt/PKB signalling is considered one element facilitating the process.[23] Indeed, shear-induced AKT phosphorylation was significantly attenuated by deletion of Scrib, whereas AKT phosphorylation in response to the flow-independent stimulus insulin was not affected. This raises the possibility that sensing of the flow forces by a Scrib-deficient endothelium is impaired (*Figure* 2B). Flow activates the mechanosensitive channel Piezo1 which, through a complex signalling pathway, eventually results in eNOS activation.[13,24] Interestingly, deletion of Scrib had no

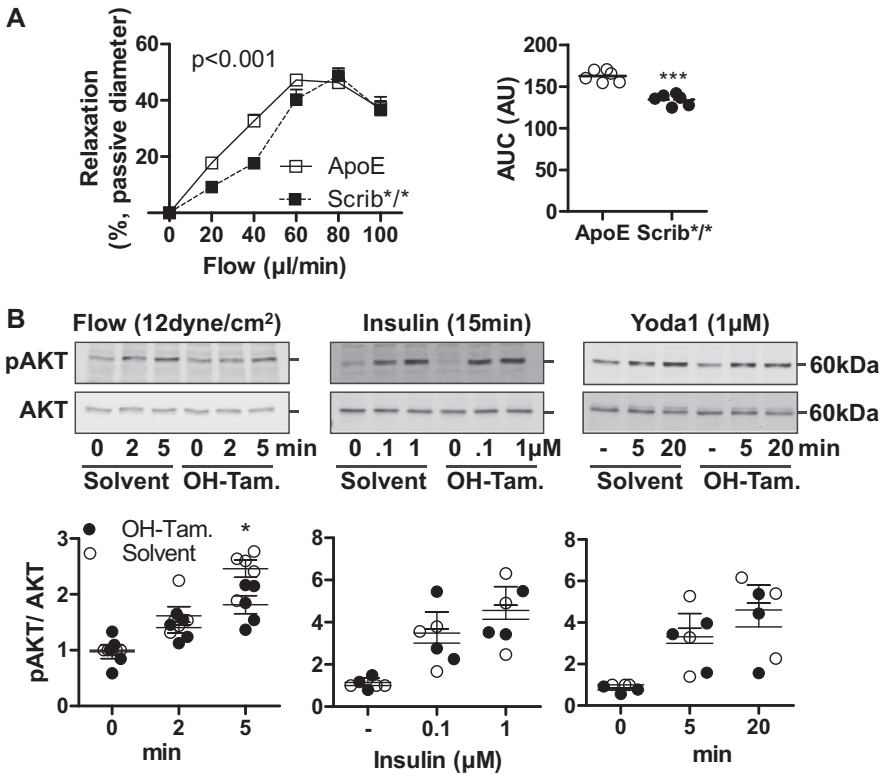

Figure 2 Role of Scrib in flow-induced dilatation and AKT phosphorylation. (*A*) Flow-induced dilatation. Mesenteric arteries from tamoxifen-treated ApoE$^{-/-}$ Scrib1-flox/flox-rosa-Cre-ERT2$^{0/0}$ (ApoE) or ApoE$^{-/-}$ Scrib1-flox/flox-rosa-Cre-ERT2$^{+/0}$ (Scrib*/*) mice were exposed to flow. Effect of a stepwise increase in perfusion flow relative to the initial diameter of vessels pre-contracted with U46619 (100 nmol/L), $n = 6$. (*B*) Role of Scrib for AKT phosphorylation. CEC were isolated from ApoE$^{-/-}$ Scrib flox/flox-Cre ERT2$^{+/0}$ mice. Scrib knockout was induced with Hydroxytamoxifen (OH-Tam., 1 µM, 2 d). Ethanol solvent controls are denoted as Solvent. CEC were either exposed to flow, $n = 5$, Insulin, $n = 3$, or Yoda, $n = 3$. Top: Representative western blots and (bottom) relative densitometry. Data represent the means ± SEM; *$P \leq 0.05$ as determined by two-way ANOVA with Bonferroni's post-hoc test, OH-Tam. vs. Solvent.

effect on the phosphorylation of AKT in response to the pharmacological Piezo1 activator Yoda1 (*Figure* 2B). This suggests that endothelial mechano-transduction is altered when Scrib is lost.

3.3 Scrib facilitates endothelial specification

An altered response to biomechanical stimuli suggests that Scrib is unlikely to mediate its effect through a single protein but rather may promote endothelial specification at large. Therefore, RNAseq, as an unbiased approach to define the endothelial specification, was performed with CEC of mice lacking the ApoE gene deletion (C57BL/6 background) and with and without tamoxifen-induced deletion of Scrib. With an adjusted *P*-value of <0.01 and a $\log_2$ fold change >1272 genes were up-regulated and 360 down-regulated in response to Scrib deletion (Supplementary material online, *Table SI*, for qRT–PCR validation see Supplementary material online, *Figure SIV*). Knockdown of Scrib affected the expression of other polarity proteins (Supplementary material online, *Figure SV*). Interestingly, Vangl2,[1] as a marker of planar cell polarity was induced by the deletion of Scrib. This induction was potentially mediated by Wnt5a[25] which was also induced. The induction of these two genes is already suggestive of a general change in the endothelial phenotype.

Gene set enrichment analysis of the top 100 up- and down-regulated genes showed strong enrichment for terms associated with development, adhesion and cancer (*Figure* 3A). The cancer term was expected as Scrib is a well-known tumour suppressor in epithelial cells.[26] In the context of tumour development, it was shown that Scrib and activated KRAS co-operate *in vivo* which leads to more aggressive lung tumours, driven by synergistic elevation in RAS-MAPK signalling.[27] The second top

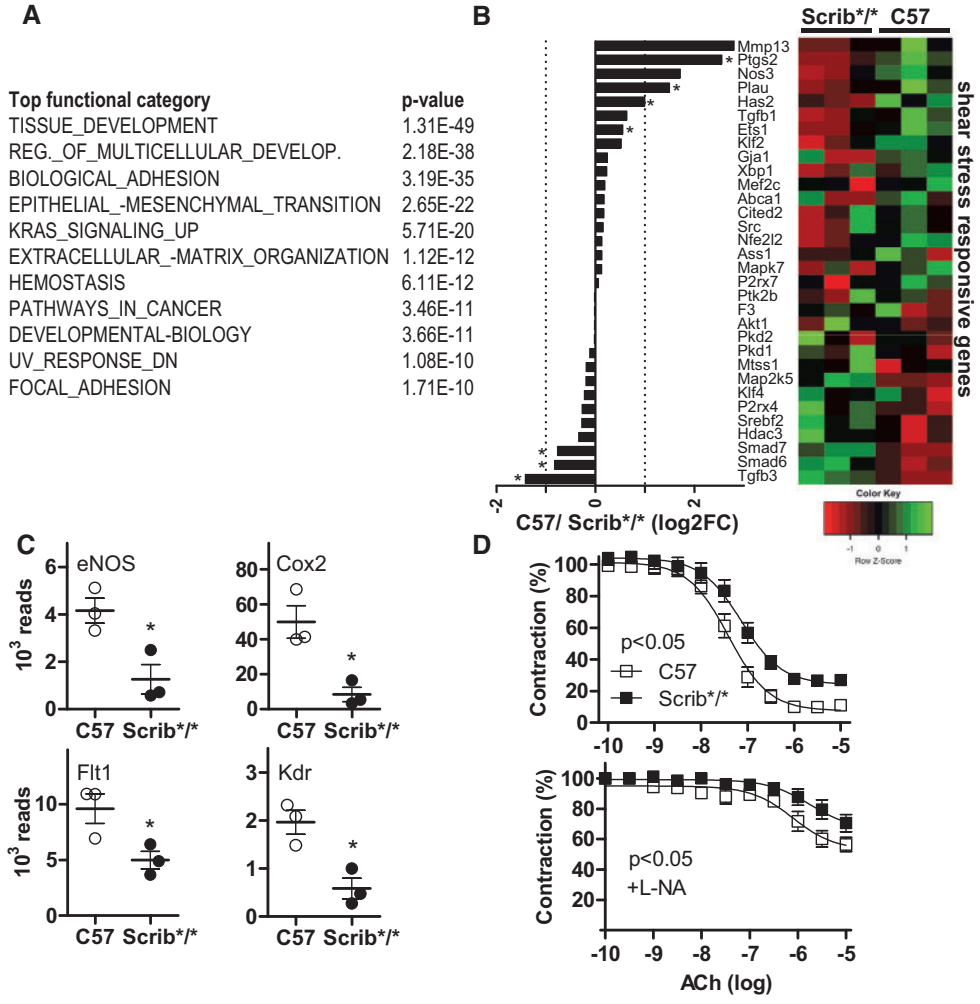

Figure 3 Role of Scrib on carotid endothelial cell gene expression and acetylcholine-induced relaxation. (*A–C*) RNA-sequencing of CEC harvested from Scrib1-flox/flox-CDH5-Cre-ERT2$^{o/0}$ (C57) and Scrib1-flox/flox-CDH5-Cre-ERT2$^{+/0}$ (Scrib*/*), $n = 3$ mice per group. All CEC were treated with Hydroxytamoxifen (1 µM, 2 d). (*A*) Gene set enrichment analysis of Scrib-regulated genes. Top 100 up- and down-regulated genes, P_{adj} <0.01 were used. The top three functional categories from GO, HALLMARK, REACTOME, and KEGG gene sets are listed. (B) $\log_2$ normalized Heat map and mean expression of genes extracted from the functional category 'shear stress responsive genes'; *P_{adj}-value ≤ 0.05. (C) Absolute expression (reads) of endothelial genes involved in endothelium-dependent relaxation, means ± SEM; *$P \leq 0.05$, *t*-test. (D) Acetylcholine-induced endothelium dependent relaxation of isolated mesenteric artery rings from tamoxifen-treated C57 and Scrib */* mice in the presence (bottom) and absence (top) of eNOS inhibition by nitro-L-arginine (L-NA, 100 µmol/L), $n = 6$. Data represent the means ± SEM; $P \leq 0.05$ as determined by two-way ANOVA for repeated measurements.

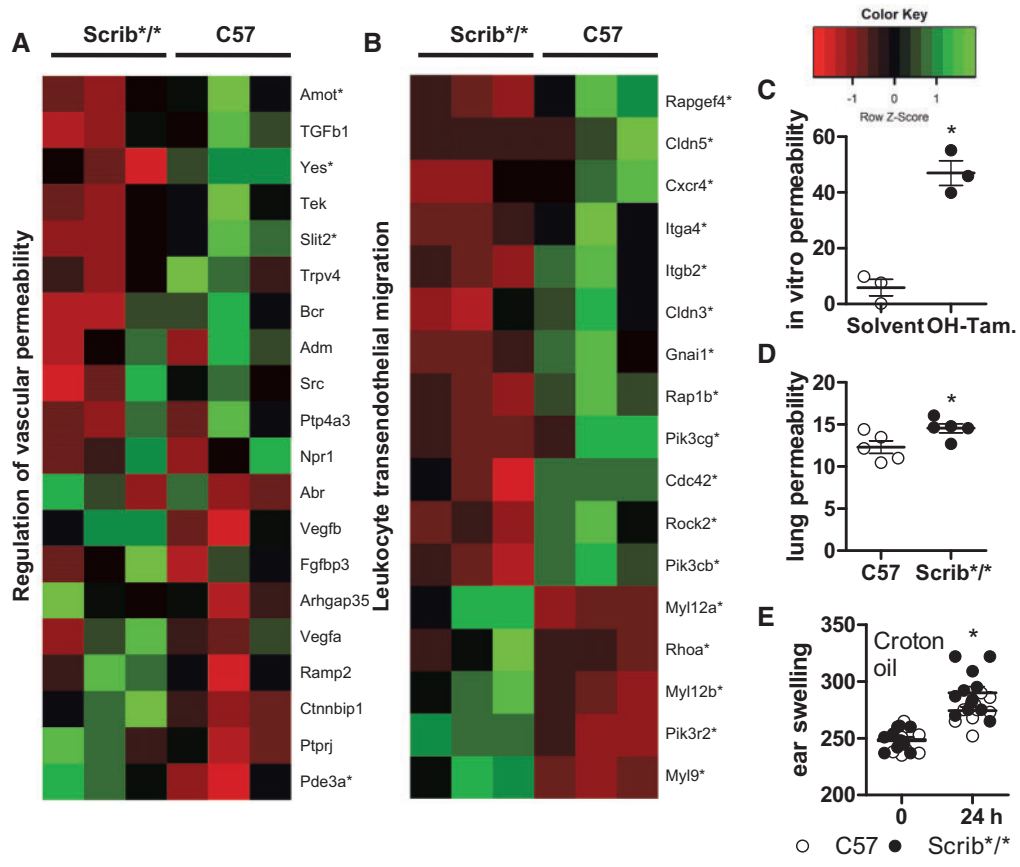

Figure 4 Role of Scrib in the control of endothelial permeability (*A, B*) Log_2 normalized Heat map of GO term genes: Regulation of vascular permeability and significantly regulated genes of the KEGG term leucocyte transendothelial migration. For RNAseq details see Figure 3 and methods part; $*P_{adj}$-value ≤ 0.05. (*C*) *In vitro* permeability assay of CEC to rhodamine isothiocyanate-dextran (1 h). CEC were isolated from tamoxifen-inducible endothelial-specific Scrib*/* mice (Scrib1-flox/flox-CDH5-Cre-ERT2$^{+/0}$). Scrib knockout was induced with Hydroxytamoxifen (OH-Tam., 1 µM, 2 d). Ethanol solvent control are denoted as Solvent, *n* = 3. (*D*) Vascular permeability of the lung as examined by Evans Blue extravasation in tamoxifen-treated endothelial-specific Scrib*/* mice or Cre negative (C57) littermates, *n* = 5. (*E*) Croton oil-induced ear oedema assay. Swelling was analysed 24 h after croton oil (1%, in acetone) application in tamoxifen-treated endothelial-specific Scrib*/* mice or Cre negative (C57) littermates, *n* = 10–12.

functional hallmark category upon Scrib knockout is epithelial to mesenchymal transition (EMT). Endothelial to mesenchymal transition (EndoMT), a special example of this process, is known to contribute to atherosclerosis development through is a special example of this process which is known to contribute to atherosclerosis development through endothelial de-specification[28] (*Figure* 3A).

When considering the EndoMT process, it is not surprising that deletion of Scrib reduced the expression of numerous endothelial signature genes and flow-responsive genes (*Figure* 3B). Among them were genes mediating endothelium-dependent relaxation in general, like those involved in endothelial autacoid synthesis and vascular endothelial growth factor (VEGF) receptors (*Figure* 3C). With such a large number of endothelial genes being differentially regulated, one could assume that Scrib-deletion-mediated impairment is not restricted to flow-sensing alone but rather to endothelial-dependent relaxation at large. Indeed, endothelial-dependent relaxation of the mesenteric artery to acetylcholine was significantly reduced in vessels of endothelial-specific Scrib-knockout animals (Scrib1-flox/flox-CDH5-Cre-ERT2$^{+/0}$) compared with vessels from WT mice. This was true not only for the NO-mediated portion but also for the relaxation mediated by prostaglandins and EDHF (*Figure* 3D).

3.4 Scrib limits permeability and macrophage extravasation

To obtain a more functional understanding of the mechanisms resulting in loss of endothelial specification after Scrib deletion, we employed a Bayesian network, which we have previously validated for atherosclerosis development.[29] After the projection of the top 100 up- and down-regulated Scrib-genes, the 'loss of Scrib' subnetwork was extracted and subjected to GO term analysis (Supplementary material online, *Figure SVI* and *Table S2*). This analysis also suggested a significant enrichment of pro-atherosclerotic pathways (adhesion, TNF alpha and TGF beta signalling, transendothelial migration) after deletion of Scrib. The gene set enrichment analysis of the Bayesian 'loss of Scrib' network (Supplementary material online, *Figure SVIB*) shows an overlap with the gene set enrichment

analysis performed with the top 100 up- and down-regulated Scrib-genes (*Figure* 3A). Interestingly, as a common denominator, the dataset pointed towards altered permeability and tissue cell recruitment as causal mechanisms for increased atherosclerosis after Scrib deletion. Based on this, we performed a re-evaluation of the RNAseq dataset. Indeed, loss of Scrib was associated with substantial changes in the expression of genes involved in vascular permeability and leucocyte migration (*Figure* 4A, B). We therefore tested permeability in cultured endothelial cells and *in vivo*. In all three approaches, loss of Scrib was associated with increased permeability (*Figure* 4C–E).

3.5 Arhgef7 is a functionally important interactor of Scrib

Scrib has no catalytic activity and thus meditates its function in polarity through protein–protein interaction. On this basis, we searched for Scrib-interacting proteins by co-IP/massspec in lysates of primary carotid artery endothelial cells. Arhgef7 (also known as βPix) and the GIT proteins were among the few, yet highly enriched interactors (*Figure 5A* and Supplementary material online, *Table S3*). These proteins are known to interact with Cdc42 and Rac1 and therefore provides an important link to the cytoskeleton, stabilization of lateral cell boarders and general cell specification.[30] Interestingly, loss of Scrib was also associated with a reduced Arhgef7 mRNA expression (*Figure* 5B), which indicates that loss of Scrib through multiple feedback loops maintains cellular specification. On the basis of these observations we tested whether Arhgef7 could be the functional link between Scrib and polarity. Knockdown of Arhgef7 reduced permeability to a similar extent as knockdown of Scrib (*Figure* 5C). This not only suggests that Arhgef7 is an important mediator of the function of Scrib but also provides a direct link between Scrib and coronary actin, which is required to stabilize lateral cell junctions. Opening of paracellular paths not only results in increased permeability but should facilitate efflux of inflammatory cells which promotes atherosclerosis development.[31] Indeed, in response to LPS treatment, macrophage extravasation to the lung was greater in endothelial-specific Scrib-knockout mice compared with control animals (*Figure* 5D).

3.6 Analysis of human plaque material suggests an anti-atherosclerotic function for Scrib in the disease context

To assess a potential importance of Scrib in the context of cardiovascular disease, we correlated the expression of Scrib with that of the other genes in 126 human carotid endarterectomy samples of the BiKE study (GSE21545).[22] Although human endarterectomy material is a complex tissue, we could confirm many of the observations of the present study in this dataset as well. Scrib exhibited a positive correlation with numerous protective genes like phospholipase A2, the flow-inducible cyclooxygenase 2 and mechanosensors like VE-Cad (Cdh5) or the VEGF-receptors Flt1 and Krd (*Figure* 6A). In contrast, genes associated with atherosclerosis and vascular dysfunction were predominantly negatively correlated with Scrib expression (*Figure* 6B).

4. Discussion

In the present study, we demonstrate that the polarity protein Scrib limits atherosclerosis development in mice. Loss of Scrib reduces endothelial autacoid release, flow sensing, and vascular permeability. Analogous to its reported effects on the EMT,[32,33] loss of Scrib had a broad effect

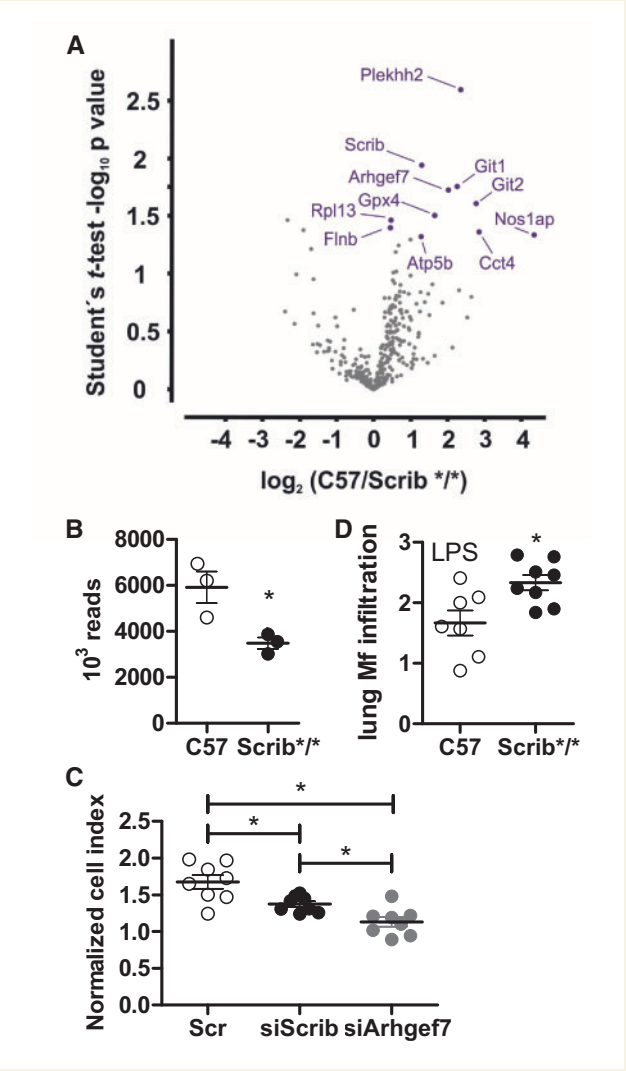

Figure 5 Arhgef7 is an interactor of Scrib. (*A*) Identification of Scrib-interacting proteins by Co-IP LC/MS. Scrib immune pull down of primary CEC isolated from Scrib1-flox/flox-Cdh5-Cre-ERT2$^{+/0}$ mice. Scrib (Scrib*/*) knockout was performed *in vitro* by induction with Hydroxytamoxifen (1 μM, 2 d) or not (C57). Scrib enriched beads with interacting proteins of control (C57, $n = 4$) and knockout (Scrib*/*, $n = 4$) were analysed by quantitative proteome analysis. Student's *t*-test significant enriched proteins (blue) were highlighted in volcano plots. (*B*) RNA-sequencing of CEC harvested from Scrib1-flox/flox-Cdh5-Cre-ERT2$^{0/0}$ (C57) and Scrib1-flox/flox-Cdh5-Cre-ERT2$^{+/0}$ (Scrib*/*), $n = 3$ mice per group. All CEC were treated with Hydroxytamoxifen (1 μM, 2 d). Absolute expression (reads) of Arhgef7, means ± SEM; $^*P \leq 0.05$, *t*-test. (*C*) Impedance analysis of endothelial barrier function. Role of Scrib or Arhgef7 down-regulation (siScrib or siArhgef7) on HUVEC. The impedance readout is expressed as 'cell index' which reflects changes in barrier function and permeability.[43] Scrambled siRNA (Scr) was used as a control. Impedance was measured in duplicate wells. Mean normalized cell index measured from 20 to 24 h after seeding cells on 96-well plates, $n = 8$. Data represent the means ± SEM; $P \leq 0.05$ as determined by one-way ANOVA for repeated measurements. (*D*) Macrophage infiltration as determined by pulmonary Emr1 mRNA content. Lipopolysaccharide (8 mg/kg) was injected intraperitoneally into tamoxifen-treated endothelial-specific Scrib*/* mice or Cre negative (C57) littermates. Two hours after injection, tissue was harvested, $n = 7$–8. Data represent the means ± SEM; $^*P \leq 0.05$, *t*-test, OH-Tam. vs. Solvent or C57 vs. Scrib*/*.

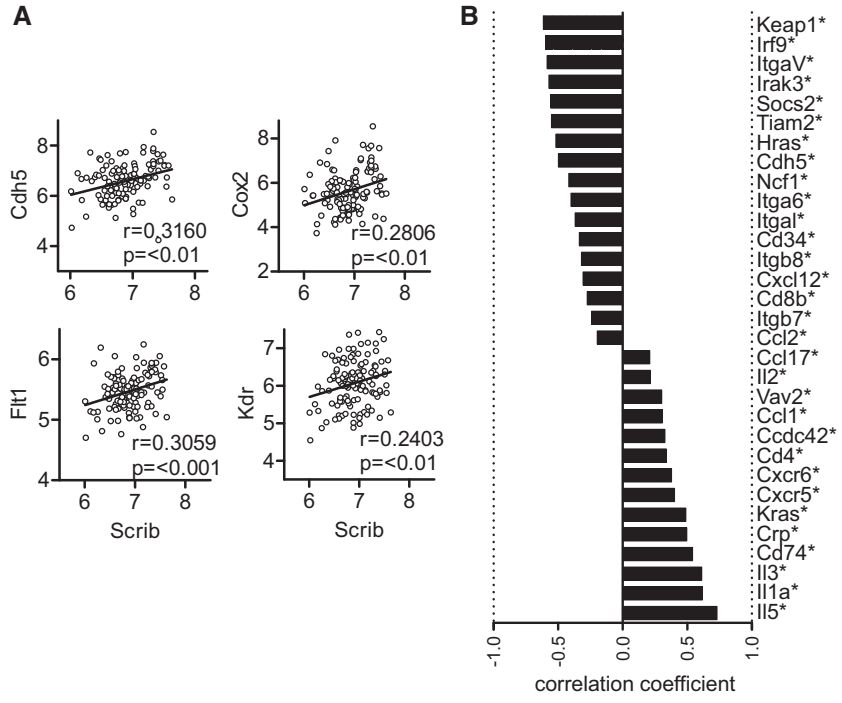

Figure 6 Pearson correlation analysis of relative Scrib mRNA expression with the mRNA expression of the genes indicated from carotid endarterectomy material of the BiKE study. (*A*) Scatter plots of representative expression correlation of the 126 human carotid plaque samples between Scrib and the genes indicated. (*B*) Selection of significant correlation as depicted by correlation coefficient; $*P_{adj.} \leq 0.05$.

on endothelial gene expression and induced endothelial to EndoMT. Thus, Scrib could be interpreted as a factor maintaining endothelial specification and differentiation. Interestingly, this view is compatible with the function of polarity proteins in epithelial cells. By establishing apico-basal polarity they allow for epithelial differentiation and promote cell specification and limit proliferation, migration, and invasion. It is therefore unsurprising that the loss of polarity of epithelial cells is associated with cancer development.

An effect of Scrib on small GTPases is well documented and several GEFs, including Arhgef7 (βPix) have been identified as protein interaction partners of Scrib in epithelial cells. A similar mechanism may be at play in endothelial cells, as also in the present study a similar subset of interacting proteins was identified in these cells. We have previously demonstrated that loss of Scrib in endothelial cells results in increased lamellipodia formation, likely as a consequence of altered Rac and Cdc42 activity.[7] Additionally, in the present study, expression of several GEFs and GTPases was altered following loss of Scrib. This aspect fits well to the increase in permeability observed in the present study. Given the complex alterations in gene expression it is unlikely that a single factor can account for the observed increased permeability, nevertheless, Arhgef7, as an important link between Scrib and cytoskeleton controlling GTPases appears to be of outstanding importance as downstream interactors of Scrib.[34] The loss of lateral junction associated with EndoMT could underlie some of this defect. For example, our data indicate that loss of Scrib in endothelial cells leads to down-regulation of Claudin 5 (Cldn5) and Slit Guidance Ligand 2 (Slit2), the ligand of Roundabout 4 (Robo4), both of which have been shown to increase vascular permeability.[35,36] We also observed an attenuation of the SDF1α-CXCR4 axis, as CXCR4 expression was reduced by Scrib deletion. The signalling of this receptor is well known to positively affect many endothelial aspects like endothelium-dependent relaxation, endothelial differentiation and to limit permeability.[36] CXCR4 is downstream of VEGF receptor signalling and, interestingly, placental growth factor (PGF), which belongs to the VEGF family and which is a VEGF receptor ligand.[37] PGF was also identified by our Bayesian network analysis as a key driver of the Scrib network. Although our network does not inform about the mechanistic links between Scrib and PGF, it is interesting to note that this growth factor also limits vascular dysfunction and promotes endothelial function.[37]

How do these functions of Scrib link to its anti-atherosclerotic property? Loss of barrier function,[31] activation of GTPases[38] and EndoMT[28] have all been shown to promote atherosclerosis. However, one of the most prominent drivers, at least in mouse models, is inflammation.[39,40] Inflammation can result from GTPase activation which regulates dedifferentiation and promotes malignant transformation.[41] Together, these various Scrib-related functions could all contribute to limit inflammatory activity and thus limit atherosclerosis development *in vivo* as observed in the present study. One previously reported property of Scrib, however, stands against this notion: we previously noted that Scrib could promote the expression of the atherosclerosis-promoting[42] adhesion molecule VCAM-1.[5] Functionally, this contributed to monocyte recruitment after TNFα treatment when ICAM-1 function was blocked by neutralizing antibodies. Importantly, here we also show in the BiKE database a significant correlation between Scrib and VCAM-1 expression. This is in contrast to the vast majority of pro-atherosclerotic factors which showed a negative correlation with Scrib not only in our murine cells but also in

human samples. It therefore appears that the interaction between Scrib and VCAM-1 is a consequence of an unusual signalling cascade involving the hardly studied transcription factor, GATA-like-protein-1.

In summary, we identified that the polarity protein Scrib maintains the endothelial phenotype and function. Loss of Scrib promoted atherosclerosis development in mice and, in human biobank material, Scrib was found to be negatively associated with factors promoting atherosclerosis.

Supplementary material

Supplementary material is available at *Cardiovascular Research* online.

Author' contributions

R.P.B. and C.S. supervised the project and edited the manuscript. C.S. performed most experiments and wrote the manuscript. F.L.D. and B.v.d.S. performed atherosclerosis experiments. K.P. and J.A.O. performed cell culture experiments. A.E.V. performed vascular reactivity studies. S.W. performed pressure myography studies. S.G. performed RNA-sequencing. E.L. and M.S.L. processed RNAseq data. J.Z. constructed the Bayesian networks. C.K. performed leucocyte migration assay. R.P.B., C.S., K.P., J.A.O., M.S.L., S.G. designed or conducted *in vitro* experiments. R.P.B., C.S., F.L.D., A.E.V., S.W., S.O., B.v.d.S., P.O.H., C.K., G.K.B., A.W., P.M., and I.W. designed or conducted *in vivo*/*ex vivo* experiments. All authors participated in editing the manuscript.

Acknowledgements

We are grateful for the excellent technical assistance of Susanne Schütz and Tanja Lüneburg. We thank Jana Meisterknecht for excellent technical assistance for sample preparation for mass spectrometry.

Conflict of interest: none declared.

Funding

This work was supported by the DFG Excellence Cluster 'Cardiopulmonary System – ECCPS', [SFB 834 (TPA2 to R.P.B)]; the Faculty of Medicine, Goethe-Universität, Frankfurt am Main, Germany and the German Center for Cardiovascular Research (DZHK), Partner site RheinMain, Frankfurt, Germany, Cardio-Pulmonary Institute (CPI), EXC 2026, Project ID: 390649896, Deutsche Forschungsgemeinschaft: SFB 815/Z1 (I.W.).

References

1. Bailly E, Walton A, Borg J-P. The planar cell polarity Vangl2 protein: from genetics to cellular and molecular functions. *Semin Cell Dev Biol* 2018;**81**:62–70.
2. St Johnston D, Ahringer J. Cell polarity in eggs and epithelia: parallels and diversity. *Cell* 2010;**141**:757–774.
3. Johnson K, Wodarz A. A genetic hierarchy controlling cell polarity. *Nat Cell Biol* 2003;**5**:12–14.
4. Chen J, Zhang M. The Par3/Par6/aPKC complex and epithelial cell polarity. *Exp Cell Res* 2013;**319**:1357–1364.
5. Kruse C, Kurz ARM, Pálfi K, Humbert PO, Sperandio M, Brandes RP, Fork C, Michaelis UR. Polarity protein Scrib facilitates endothelial inflammatory signaling. *Arterioscler Thromb Vasc Biol* 2015;**35**:1954–1962.
6. Zhou J, Li Y-S, Chien S. Shear stress-initiated signaling and its regulation of endothelial function. *Arterioscler Thromb Vasc Biol* 2014;**34**:2191–2198.
7. Michaelis UR, Chavakis E, Kruse C, Jungblut B, Kaluza D, Wandzioch K, Manavski Y, Heide H, Santoni M-J, Potente M, Eble JA, Borg J-P, Brandes RP. The polarity protein Scrib is essential for directed endothelial cell migration. *Circ Res* 2013;**112**:924–934.
8. Pearson HB, McGlinn E, Phesse TJ, Schlüter H, Srikumar A, Gödde NJ, Woelwer CB, Ryan A, Phillips WA, Ernst M, Kaur P, Humbert P. The polarity protein Scrib mediates epidermal development and exerts a tumor suppressive function during skin carcinogenesis. *Mol Cancer* 2015;**14**:169.
9. Hoyer FF, Khoury M, Slomka H, Kebschull M, Lerner R, Lutz B, Schott H, Lütjohann D, Wojtalla A, Becker A, Zimmer A, Nickenig G. Inhibition of endocannabinoid-degrading enzyme fatty acid amide hydrolase increases atherosclerotic plaque vulnerability in mice. *J Mol Cell Cardiol* 2014;**66**:126–132.
10. Schürmann C, Rezende F, Kruse C, Yasar Y, Löwe O, Fork C, van de Sluis B, Bremer R, Weissmann N, Shah AM, Jo H, Brandes RP, Schröder K. The NADPH oxidase Nox4 has anti-atherosclerotic functions. *Eur Heart J* 2015;**36**:3447–3456.
11. GöRlach A, Brandes RP, Nguyen K, Amidi M, Dehghani F, Busse R. A gp91phox containing NADPH oxidase selectively expressed in endothelial cells is a major source of oxygen radical generation in the arterial wall. *Circ Res* 2000;**87**:26–32.
12. Wang S, Iring A, Strilic B, Albarrán Juárez J, Kaur H, Troidl K, Tonack S, Burbiel JC, Müller CE, Fleming I, Lundberg JO, Wettschureck N, Offermanns S. $P2Y_2$ and Gq/G_{11} control blood pressure by mediating endothelial mechanotransduction. *J Clin Invest* 2015;**125**:3077–3086.
13. Wang S, Chennupati R, Kaur H, Iring A, Wettschureck N, Offermanns S. Endothelial cation channel PIEZO1 controls blood pressure by mediating flow-induced ATP release. *J Clin Invest* 2016;**126**:4527–4536.
14. Fleming I, Fisslthaler B, Dixit M, Busse R. Role of PECAM-1 in the shear-stress-induced activation of Akt and the endothelial nitric oxide synthase (eNOS) in endothelial cells. *J Cell Sci* 2005;**118**:4103–4111.
15. Davis MPA, van Dongen S, Abreu-Goodger C, Bartonicek N, Enright AJ. Kraken: a set of tools for quality control and analysis of high-throughput sequence data. *Methods* 2013;**63**:41–49.
16. Dobin A, Davis CA, Schlesinger F, Drenkow J, Zaleski C, Jha S, Batut P, Chaisson M, Gingeras TR. STAR: ultrafast universal RNA-seq aligner. *Bioinformatics* 2013;**29**:15–21.
17. Liao Y, Smyth GK, Shi W. featureCounts: an efficient general purpose program for assigning sequence reads to genomic features. *Bioinformatics* 2014;**30**:923–930.
18. Love MI, Huber W, Anders S. Moderated estimation of fold change and dispersion for RNA-seq data with DESeq2. *Genome Biol* 2014;**15**:550.
19. Shiri-Sverdlov R, Wouters K, van Gorp PJ, Gijbels MJ, Noel B, Buffat L, Staels B, Maeda N, van Bilsen M, Hofker MH. Early diet-induced non-alcoholic steatohepatitis in APOE2 knock-in mice and its prevention by fibrates. *J Hepatol* 2006;**44**:732–741.
20. Rappsilber J, Mann M, Ishihama Y. Protocol for micro-purification, enrichment, pre-fractionation and storage of peptides for proteomics using StageTips. *Nat Protoc* 2007;**2**:1896–1906.
21. Cox J, Mann M. MaxQuant enables high peptide identification rates, individualized p.p.b.-range mass accuracies and proteome-wide protein quantification. *Nat Biotechnol* 2008;**26**:1367–1372.
22. Folkersen L, Persson J, Ekstrand J, Agardh HE, Hansson GK, Gabrielsen A, Hedin U, Paulsson-Berne G. Prediction of ischemic events on the basis of transcriptomic and genomic profiling in patients undergoing carotid endarterectomy. *Mol Med* 2012;**18**:669–675.
23. Busse R, Fleming I. Regulation of endothelium-derived vasoactive autacoid production by hemodynamic forces. *Trends Pharmacol Sci* 2003;**24**:24–29.
24. Hyman AJ, Tumova S, Beech DJ. Piezo1 channels in vascular development and the sensing of shear stress. *Curr Top Membr* 2017;**79**:37–57.
25. Shi Y-N, Zhu N, Liu C, Wu H-T, Gui Y, Liao D-F, Qin L. Wnt5a and its signaling pathway in angiogenesis. *Clin Chim Acta* 2017;**471**:263–269.
26. Pearson HB, Perez-Mancera PA, Dow LE, Ryan A, Tennstedt P, Bogani D, Elsum I, Greenfield A, Tuveson DA, Simon R, Humbert PO. SCRIB expression is deregulated in human prostate cancer, and its deficiency in mice promotes prostate neoplasia. *J Clin Invest* 2011;**121**:4257–4267.
27. Elsum IA, Yates LL, Pearson HB, Phesse TJ, Long F, O'Donoghue R, Ernst M, Cullinane C, Humbert PO. Scrib heterozygosity predisposes to lung cancer and cooperates with KRas hyperactivation to accelerate lung cancer progression in vivo. *Oncogene* 2014;**33**:5523–5533.
28. Gong H, Lyu X, Wang Q, Hu M, Zhang X. Endothelial to mesenchymal transition in the cardiovascular system. *Life Sci* 2017;**184**:95–102.
29. Hitzel J, Lee E, Zhang Y, Bibli SI, Li X, Zukunft S, Pflüger B, Hu J, Schürmann C, Vasconez AE, Oo JA, Kratzer A, Kumar S, Rezende F, Josipovic I, Thomas D, Giral H, Schreiber Y, Geisslinger G, Fork C, Yang X, Sigala F, Romanoski CE, Kroll J, Jo H, Landmesser U, Lusis AJ, Namgaladze D, Fleming I, Leisegang MS, Zhu J, Brandes RP. Oxidized phospholipids regulate amino acid metabolism through MTHFD2 to facilitate nucleotide release in endothelial cells. *Nat Commun* 2018;**9**:2292.
30. Zhou W, Li X, Premont RT. Expanding functions of GIT Arf GTPase-activating proteins, PIX Rho guanine nucleotide exchange factors and GIT-PIX complexes. *J Cell Sci* 2016;**129**:1963–1974.
31. Chistiakov DA, Orekhov AN, Bobryshev YV. Endothelial barrier and its abnormalities in cardiovascular disease. *Front Physiol* 2015;**6**:365.
32. Elsum IA, Martin C, Humbert PO. Scribble regulates an EMT polarity pathway through modulation of MAPK-ERK signaling to mediate junction formation. *J Cell Sci* 2013;**126**:3990–3999.
33. Yamben IF, Rachel RA, Shatadal S, Copeland NG, Jenkins NA, Warming S, Griep AE. Scrib is required for epithelial cell identity and prevents epithelial to mesenchymal transition in the mouse. *Dev Biol* 2013;**384**:41–52.
34. Wilson E, Leszczynska K, Poulter NS, Edelmann F, Salisbury VA, Noy PJ, Bacon A, Rappoport JZ, Heath JK, Bicknell R, Heath VL. RhoJ interacts with the GIT-PIX complex and regulates focal adhesion disassembly. *J Cell Sci* 2014;**127**:3039–3051.

35. Ma S-C, Li Q, Peng J-Y, Zhouwen J-L, Diao J-F, Niu J-X, Wang X, Guan X-D, Jia W, Jiang W-G. Claudin-5 regulates blood-brain barrier permeability by modifying brain microvascular endothelial cell proliferation, migration, and adhesion to prevent lung cancer metastasis. *CNS Neurosci Ther* 2017;**23**:947–960.
36. Döring Y, Noels H, van der Vorst EPC, Neideck C, Egea V, Drechsler M, Mandl M, Pawig L, Jansen Y, Schröder K, Bidzhekov K, Megens RTA, Theelen W, Klinkhammer BM, Boor P, Schurgers L, van Gorp R, Ries C, Kusters PJH, van der Wal A, Hackeng TM, Gäbel G, Brandes RP, Soehnlein O, Lutgens E, Vestweber D, Teupser D, Holdt LM, Rader DJ, Saleheen D, Weber C. Vascular CXCR4 limits atherosclerosis by maintaining arterial integrity: evidence from mouse and human studies. *Circulation* 2017;**136**:388–403.
37. Dewerchin M, Carmeliet P. PlGF: a multitasking cytokine with disease-restricted activity. *Cold Spring Harb Perspect Med* 2012;**2**:a011056.
38. Amerongen G. P V N, Vermeer MA, Nègre-Aminou P, Lankelma J, Emeis JJ, van Hinsbergh VWM. Simvastatin improves disturbed endothelial barrier function. *Circulation* 2000;**102**:2803–2809.
39. Ross R. Atherosclerosis—an inflammatory disease. *N Engl J Med* 1999;**340**:115–126.
40. Ridker PM, Everett BM, Thuren T, MacFadyen JG, Chang WH, Ballantyne C, Fonseca F, Nicolau J, Koenig W, Anker SD, Kastelein JJP, Cornel JH, Pais P, Pella D, Genest J, Cifkova R, Lorenzatti A, Forster T, Kobalava Z, Vida-Simiti L, Flather M, Shimokawa H, Ogawa H, Dellborg M, Rossi PRF, Troquay RPT, Libby P, Glynn RJ. Antiinflammatory therapy with canakinumab for atherosclerotic disease. *N Engl J Med* 2017;**377**:1119–1131.
41. Hanahan D, Weinberg RA. Hallmarks of cancer: the next generation. *Cell* 2011;**144**:646–674.
42. Nakashima Y, Raines EW, Plump AS, Breslow JL, Ross R. Upregulation of VCAM-1 and ICAM-1 at atherosclerosis-prone sites on the endothelium in the ApoE-deficient mouse. *Arterioscler Thromb Vasc Biol* 1998;**18**:842–851.
43. Monaghan-Benson E, Wittchen ES. In vitro analyses of endothelial cell permeability. *Methods Mol Biol* 2011;**763**:281–290.